0026-895X/04/6504-1016–1028$20.00
MOLECULAR PHARMACOLOGY
Copyright © 2004 The American Society for Pharmacology and Experimental Therapeutics
Mol Pharmacol 65:1016–1028, 2004

Vol. 65, No. 4
2859/1142940
Printed in U.S.A.

MOL PHARM
MOLECULAR PHARMACOLOGY

Differential Susceptibilities of Murine Hepatoma 1c1c7 and Tao Cells to the Lysosomal Photosensitizer NPe6: Influence of Aryl Hydrocarbon Receptor on Lysosomal Fragility and Protease Contents

Joseph A. Caruso, Patricia A. Mathieu, Aby Joiakim, Brendan Leeson, David Kessel, Bonnie F. Sloane, and John J. Reiners, Jr.

Institute of Environmental Health Sciences (J.A.C., P.A.M., A.J., J.J.R.), Wayne State University, Detroit, Michigan and Department of Pharmacology (B.L., D.K., B.F.S.), Wayne State University School of Medicine, Detroit, Michigan

Received July 20, 2003; accepted January 20, 2004

This article is available online at http://molpharm.aspetjournals.org

ABSTRACT

Irradiation of murine hepatoma 1c1c7 cultures presensitized with *N*-aspartyl chlorin e6 (NPe6) caused lysosomal disruption and apoptosis. Tao cells, a variant of the 1c1c7 line having lower aryl hydrocarbon receptor (AhR) contents, were resistant to the pro-apoptotic effects of NPe6 in the same photodynamic therapy protocol. Colony-forming assays were used to establish light dose-dependent and NPe6 concentration-dependent cytotoxicity curves. Lysosomal breakage and cell survival paralleled one another in both cell types. When analyzed at comparable lethal dose conditions, the onset of apoptosis was delayed, and the magnitude of the apoptotic response was muted in Tao cells, as assessed by morphology, annexin V binding, caspase-3 activities, and analyses of Bid, pro-caspase-9, and pro-caspase-3 cleavage. In contrast, the kinetics/magnitude of pro-caspase-3 activation in the two cell lines were identical after exposure to HA14–1 or Jo2 antibody, inducers of the intrinsic and extrinsic apoptotic pathways, respectively. Tao endosomal/lysosomal extracts contained ~50%, 35%, and 55% of the Bid cleavage and cathepsin B and D activities of 1c1c7 endosomes/lysosomes, respectively. Western blot analyses confirmed reduced cathepsin B/D contents in Tao cells. Analyses of 1c1c7/Tao variants engineered to express antisense/sense AhR constructs suggested that endosomal/lysosomal cathepsin B and D content, but not whole cell content, correlated with AhR expression. These studies provide a mechanism for the resistance of Tao cultures to the pro-apoptotic effects of a protocol causing targeted disruption of lysosomes. They also suggest that the AhR, in the absence of exogenous ligand, may affect the trafficking/processing of proteases normally found in endosomes/lysosomes.

Photodynamic therapy (PDT) is a procedure that uses light to activate photosensitizers and generate singlet oxygen. PDT is used to destroy tumors and in the treatment of macular degeneration and atherosclerotic plaque (Dougherty et al., 1998). Numerous agents function as photosensitizers in PDT protocols and accumulate in specific organelles. The photosensitizer *N*-aspartyl chlorin e6 (NPe6) preferentially accumulates in lysosomes and causes lysosomal disruption after irradiation (Kessel et al., 2000; Reiners et al., 2002). Surprisingly, PDT-mediated lysosomal disruption leads to apoptosis, as opposed to necrosis, in several cell types (Kessel et al., 2000). In the case of murine hepatoma 1c1c7 cells, NPe6-mediated disruption of lysosomes in PDT protocols results in the sequential cleavage/activation of Bid, release of cytochrome *c* from mitochondria, and subsequent activations of pro-caspase-9 and downstream caspases (Reiners et al., 2002). Released lysosomal proteases presumably initiate the apoptotic response because lysosomes contain a protease capable of cleaving/activating Bid (Stoka et al., 2001; Reiners et al., 2002).

In current paradigms the aryl hydrocarbon receptor (AhR) is generally depicted as a cytosolic, ligand-activated transcription factor (Hahn, 1998; Whitlock, 1999; Gu et al., 2000).

This work was supported by National Institutes of Health Grant ES009392 and a pilot grant awarded by the P30-ES006639-supported Toxicology Center at Wayne State University. The project was assisted by the services of the Cell Culture and Imaging and Cytometry Facility Cores, which were supported by National Institute of Environmental Health Sciences grant P30-ES006639.

ABBREVIATIONS: PDT, photodynamic therapy; NPe6, *N*-aspartyl chlorin e6; AhR, aryl hydrocarbon receptor; TNF, tumor necrosis factor; Ac-, *N*-acetyl-; AMC, amino-4-methylcoumarin; Z-, *N*-benzyloxycarbonyl-; CA-074, L-3-*trans*-(propylcarbamoyl)oxirane-2-carbonyl-L-isoleucyl-L-proline; HA14–1, ethyl 2-amino-6-bromo-4-(1-cyano-2-ethoxy-2-oxoethyl)-4H-chromene-3-carboxylate; PBS, phosphate-buffered saline; FACS, fluorescence-activated cell sorting; FITC, fluorescein isothiocyanate; MES, 2-[*N*-morpholino]ethanesulfonic acid; ECL, enhanced chemiluminescence; AO, acridine orange; PI, propidium iodide; $\Delta\Psi_m$, mitochondrial membrane potential.

Downloaded from molpharm.aspetjournals.org by guest on December 1, 2012

MOL PHARM

MOLECULAR PHARMACOLOGY

Upon ligand binding, the AhR translocates to the nucleus, where it complexes with the aryl hydrocarbon receptor nuclear translocator and other coactivating or corepressing proteins. The resulting complexes subsequently interact with specific enhancer sequences in target genes designated dioxin-responsive elements. This interaction can either negatively or positively regulate the transcription of target genes (Hankinson, 1995; Dong et al., 1997; Sulentic et al., 2000).

The cellular functions of the AhR have been defined by comparing the effects of AhR ligands in wild-type and AhR-null mice or cell lines. Such approaches have documented the role of the AhR in mediating the cytostatic, cytotoxic, and teratogenic effects of 2,3,7,8-tetrachlorodibenzo-*p*-dioxin, a potent AhR ligand (Gonzalez and Fernandez-Salguero, 1998). Comparative studies have also defined the role of the AhR in the 2,3,7,8-tetrachlorodibenzo-*p*-dioxin–induced transcriptional activation of several phase I and II biotransformation genes (Gonzalez and Fernandez-Salguero, 1998). Although the ligand-mediated functions of the AhR have received considerable attention, recent studies suggest that the AhR may also have ligand-independent functions. Specifically, AhR-null mice develop liver fibrosis and a cardiomyopathy not seen in wild-type AhR-containing mice (Fernandez-Salguero et al., 1997). AhR-null or -deficient cell lines generally have lengthened doubling times and a more spindly morphology than their wild-type counterparts (Ma and Whitlock, 1996; Reiners and Clift, 1999; Elizondo et al., 2000). In addition, AhR content seems to regulate susceptibility to different classes of apoptotic inducers in cells of the murine hepatoma 1c1c7 lineage. Whereas 1c1c7 cells undergo apoptosis after exposure to cell-permeable, short-chain ceramide analogs, AhR-deficient variant lines (Tao, WARV) die primarily by a necrotic process (Reiners and Clift, 1999). In contrast, AhR content did not influence susceptibility to and development of apoptosis after exposure to staurosporine or doxorubicin (Reiners and Clift, 1999).

Recent studies have documented the disruption/permeabilization of lysosomes in cultured hepatocyes after exposure to an apoptotic concentration of TNFα (Guicciardi et al., 2000; Foghsgaard et al., 2001; Werneburg et al., 2002). Pharmacological inhibition of either sphingomyelinases or ceramidases, enzymes involved in the generation of ceramide and its conversion to sphingosine, ablated TNFα-mediated lysosomal damage and apoptosis (Ségui et al., 2001; Colell et al., 2002; Luberto et al., 2002). Although unproven, the lysosomal disruption noted in these studies may reflect the actions of sphingosine and its functioning as a lysosomal detergent (Kagedal et al., 2001; Werneburg et al., 2002). Given the roles of ceramide and lysosomes in the above model of TNFα-induced apoptosis, and our prior demonstration that lysosomal proteases can activate the intrinsic apoptotic pathway via cleavage of Bid, we hypothesized that differences in lysosomal Bid cleavage activities might account for the differential sensitivities of AhR wild-type 1c1c7 and AhR-deficient Tao cells to the pro-apoptotic effects of ceramide. To test this hypothesis, we used NPe6 and PDT to cause a targeted disruption of the lysosomes in 1c1c7 and Tao cells and monitored the development of apoptosis. Such studies showed that the development of apoptosis was delayed and muted in Tao cells after PDT and that Tao lysosomes/endosomes had lower Bid cleavage activities than the corresponding organelles from 1c1c7 cells. Moreover, the lysosomal/endosomal contents/activities of multiple proteases/hydrolases were also reduced in Tao cells. Analyses of variant cell lines showed that these differences correlated with cellular AhR content.

Materials and Methods

Chemicals. NPe6 was the gift of Light Sciences Corp. (Issaquah, WA). Fluorescent probes for lysosomal integrity (acridine orange) and chromatin condensation (HO33342) were purchased from Molecular Probes (Eugene, OR). Ac-DEVD-AMC and Jo2 Armenian hamster IgG (azide and endotoxin free) were purchased from BD Biosciences (San Diego, CA). Pepstatin A and AMC were purchased from Calbiochem (La Jolla, CA). The cathepsin B substrate Z-RR-AMC and the cathepsin D substrate Ac-ED(Edans)KPILFFRLGK-(Dabcyl)E-NH_2, and the cathepsin D substrate standard Ac-RE(Edans)-A-NH_2 were purchased from Bachem Bioscience Inc. (King of Prussia, PA). CA074 was obtained from Peptides International, Inc. (Louisville, KY). HA14–1 was purchased from Ryan Scientific, Inc. (Isle of Palms, SC). Recombinant murine Bid was obtained from R&D Systems, Inc. (Minneapolis, MN). Bicinchoninic acid was purchased from Sigma-Aldrich (St. Louis, MO).

Cell Culture. Murine hepatoma Hepa 1c1c7, Tao, TCMV, TAHR, WCMV, and WARV cell lines were obtained from Dr. J. P. Whitlock, Jr. (Stanford University, Stanford, CA). All cell lines were grown in α-minimum essential medium supplemented with 5% fetal bovine serum and antibiotics in a 5% CO_2 atmosphere, at 37°C, either in culture dishes or on 12-mm glass coverslips coated with poly-L-lysine. The growth medium used for the culturing of TCMV, TAHR, WCMV, and WARV cells was also supplemented with 500 ng/ml of G418. The derivation of these four cell lines has been described previously (Ma and Whitlock, 1996). All cell lines were plated at densities that ensured exponential growth 3 days after plating. Medium was always changed 2 days after plating. Treatments were always performed with 3-day-old cultures.

PDT Protocols. Subconfluent monolayers were washed twice with PBS before being refed with complete medium containing NPe6. Solutions of NPe6 were always prepared immediately before use from dried power and made in sterile water. After a loading period of ~45 to 60 min, the cultures were washed three times with PBS, refed, and then irradiated. Cultures loaded with NPe6 were irradiated for various lengths of time at 22°C using a 600-W quartz-halogen lamp with IR radiation attenuated by a 100-cm layer of water and an 850-nm cutoff filter. The bandwidth was further confined to 650 to 700 nm by a broadband interference filter. Light intensity at wavelengths of NPe6 absorbance was 1.5 mW/cm^2. Hence, 1 s of irradiation = 1.5 mJ/cm^2.

NPe6 Loading Analyses. Subconfluent monolayers of 3-day-old cultures grown in 35-mm culture dishes were washed three times with PBS and refed with complete medium containing different concentrations of NPe6. After 30, 60, and 120 min, cultures were washed three times with PBS and flooded with 1.5 ml of H_20 containing 0.5% Triton X-100. After 5 to 10 min at room temperature, the cells were scraped with a rubber policeman and transferred to a conical tube. Plates were washed once with an additional 1.5 ml of the Triton X-100 solution, and the washes were added to the original lysates. Parallel plates were treated with trypsin/EDTA, and cell numbers were determined with a hemocytometer. Cellular NPe6 contents were determined by analyses of the fluorescence signature of NPe6. Specifically, lysates were excited at 400 nm and fluorescence emission was determined with an Instaspec IV charge-coupled device (Oriel Corp., Stratford, CT), coupled to a monochronometer, which was set for a 0.5-s scan in single-scan mode. Fluorescence emission was attenuated by a 630-nm cutoff filter to omit any extraneous porphyrin signatures. Emission spectra were read at their peaks (~660 nm), and recorded in fluorescence units. The 0.5% Triton X-100 solution was used to establish a baseline. NPe6 content per cell is expressed as fluorescence units per 10^3 cells.

Downloaded from molpharm.aspetjournals.org by guest on December 1, 2012

aspet

MOL PHARM

MOLECULAR PHARMACOLOGY

Fluorescence Microscopy of Lysosomes and Nuclei. Nuclear morphology was assessed by labeling adherent cells for 10 min at 37°C with HO33342 (5 μM). Cultures were then washed three times with PBS and observed by fluorescence microscopy using excitation at 330 to 380 nm and measuring fluorescence at 420 to 450 nm. The same cultures were simultaneously loaded with 0.5 μM AO to image lysosomes. The wavelengths for acquiring AO fluorescence were excitation at 400 to 440 nm and emission at 590 to 650 nm.

FACS Analyses of Acridine Orange-Labeled Lysosomes. Subconfluent cultures were incubated with AO (8 μM) for 20 min at 37°C before being washed three times with PBS and detached by incubation with trypsin/EDTA. Cell suspensions were transferred to a 15-ml conical tube and diluted with Dulbecco's modified Eagles's medium/Ham's F-12 medium containing 5% horse serum, and pelleted by centrifugation; the pellet was subsequently washed once with PBS and resuspended in the same medium without serum. Cell suspensions were immediately analyzed by flow cytometry on a FACSCalibur instrument (BD Biosciences, San Jose, CA). A threshold was set on the basis of forward and 90° side scatter that voided the counting of debris, and a gate was set that counted the bulk of the cell population (~95–98% of all detected events above the threshold). Red AO fluorescence (FL3, PerCP detector) was collected for 20,000 cells in the gated population. Four cultures of each cell line were analyzed. Flow cytometry histograms were analyzed with Cell Quest software (BD Biosciences).

FACS Analyses of Annexin V Binding. After transfer of culture medium to a 15-ml conical tube, cultures were washed twice with PBS and the washings were added to the culture medium. Adherent cells were released with trypsin/EDTA and transferred to the tube containing culture medium and washings. Cells, debris, and apoptotic bodies were pelleted by centrifugation and then washed once with PBS. The washed pellet was subsequently labeled with annexin V and propidium iodide as described by the manufacturer of the Annexin V-FITC apoptosis detection kit (Oncogene Research Products, Boston, MA). Cells were immediately analyzed by flow cytometry on a FACSCalibur instrument. On the basis of forward and 90° side scatter, a threshold was set that voided the counting of debris, and a gate was set that counted cells but not apoptotic bodies. The FITC signal of annexin V was detected at 518 nm by FL1 (FITC detector), and propidium iodide fluorescence was detected at 620 nm by FL2 (phycoerythrin fluorescence detector).

Effects of PDT on Cell Viability. Subconfluent cultures were detached by incubation with trypsin/EDTA, washed, and subsequently suspended in culture medium and plated (400–1000 cells/plate). NPe6 was added ~16 to 18 h after plating. After ~45 min, the cultures were washed three times with PBS and refed immediately before irradiation. After irradiation, cultures were returned to a humidified 5% CO_2 chamber and incubated at 37°C. The medium was changed every 3 days, and colonies were scored 8 to 10 days after plating. Previous studies have shown that only a low percentage of Hepa 1c1c7 cells divide in the first 20 h after passaging.

DEVDase Assay. Cultures were washed twice with PBS before being flooded with lysis buffer (solution A: 10 mM Tris, pH 7.5, 130 mM NaCl, 1% Triton X-100, 10 mM NaF, 10 mM NaP_i, and 10 mM $NaPP_i$). Cells in culture medium and PBS washes were pooled, washed with PBS, and pelleted by centrifugation. After ~3 to 10 min of incubation on ice, culture dishes were scraped and the lysate was added to the cell pellet derived from the culture medium. The lysate was then transferred to a small tube, sonicated for 1 s, and centrifuged at 13,000*g* for 10 min. Supernatant fluids were aliquoted and stored at −80°C. The procedure for assay of DEVDase using Ac-DEVD-AMC as substrate has been described in detail (Reiners and Clift, 1999). The only deviation from the protocol was that assay mixtures were scaled for 96-well plates. Changes in fluorescence over time were converted into picomoles of product by comparison with a standard curve made with AMC. DEVDase specific activities are reported as nanomoles of product per minute per milligram of protein. The bicinchoninic acid assay, using bovine serum albumin as a standard, was used to estimate protein concentrations.

Preparation of Cytosol for Bid Cleavage Assays. Cells were released from culture dishes with trypsin/EDTA, mixed with α-minimum essential medium plus 5% fetal bovine serum, and pelleted by centrifugation. The pellet (~10^8 cells) was sequentially washed once with PBS and once with 0.25 M sucrose. After centrifugation, the washed pellet was resuspended in 1 ml of 0.25 M sucrose and homogenized with a Dounce tissue grinder (Wheaton, Millville, NJ) using 15 strokes. The resulting homogenate was sequentially centrifuged at 14,000*g* for 5 min and 100,000*g* for 1 h. The final supernatant fluid represented 'cytosol' and was aliquoted and stored at −80°C.

Preparation of Lysosomal Extracts for in Vitro Cleavage Assays. The procedures used for the isolation and disruption of lysosomes used for in vitro Bid cleavage assays have been described in detail (Reiners et al., 2002).

In Vitro Bid Cleavage Assay. For the studies reported in Fig. 9A, cytosol (10 μg) was incubated with or without 2 μg of lysosomal extract at 37°C, in a 30-μl reaction mixture containing 100 μM sodium acetate, pH 5.5, 10% glycerol, and 2 mM dithiothreitol. For the studies reported in Fig. 9B, various amounts of lysosomal extract were incubated with 40 ng of recombinant murine Bid at 37°C in a 20-μl reaction mixture containing 10 mM MES, pH 5.5. In both protocols, the reactions were terminated by the addition of SDS PAGE loading buffer. Bid and tBid in these studies were detected by Western blotting using the conditions reported previously by Reiners et al. (2002). The primary antibody used for the detection of Bid/tBid in these studies was a rabbit polyclonal antibody made to full-length recombinant murine Bid (gift of X-M Yin, University of Pittsburgh School Medicine, Pittsburgh, PA).

Western Blot Analyses. Lysates of whole cells were prepared with solution A supplemented 1/10 (v:v) with a 10× solution of protease inhibitor cocktail (Sigma), sonicated for 1 s, and centrifuged at 13,000*g* for 5 min. Lysosomal lysates were prepared by incubating lysosomes with 0.25 M sucrose, 25 mM MES, pH 6.5, 1 mM EDTA, and 0.1% Triton X-100 for 1 min, followed by centrifugation at 13,000*g* for 5 min. Supernatant fluids were aliquotted and stored at −80°C. Polypeptides in supernatant fluids were separated on 8% (AhR), 12.5% (cathepsins B and D), or 15% (Bid, caspase-3, and caspase-9) polyacrylamide-SDS gels and electrophoretically transferred onto nitrocellulose. After transfer, the blots were incubated with blocking solution (5% Carnation dehydrated nonfat milk in PBS/0.05% Tween 20) for 2 h at room temperature. Blocked blots were washed with PBS/0.05% Tween 20 and subsequently incubated overnight at room temperature with rabbit polyclonal antibodies raised to the murine AhR (BioMol Research Laboratories, Plymouth Meeting, PA), murine caspase-9 (Cell Signaling Technology, Beverly, MA), human caspase-3 (Santa Cruz Biotechnology, Inc., Santa Cruz, CA), human cathepsin D (Oncogene Research Products), full-length recombinant human cathepsin B (generated in-house), or murine Bid (Cell Signaling Technology). Primary rabbit antibodies were detected by a 1.5-h incubation, at room temperature, with a horseradish peroxidase-linked donkey anti-rabbit IgG (Amersham Biosciences, Piscataway, NJ). Primary and secondary antibody dilutions were made with PBS/0.05% Tween 20 containing 2.5% Carnation dehydrated nonfat milk. Immune complexes were visualized with an ECL detection kit (Amersham Pharmacia Biotech, Inc.) and recorded on X-ray film. Band intensities were quantitified using Scion Image Densitometric Analyses software (Scion Corporation, Frederick, MD).

Cathepsin Assays. The fluorometric assays used for the measurement of whole cell and lysosomal cathepsin B and D activities have been described in detail (Guo et al., 2002; Reiners et al., 2002). Z-RR-AMC and Ac-ED(Edans)KPILFFRLGK(Dabcyl)E-NH_2 were used as substrates in cathepsin B and D assays, respectively. Contributions of cathepsin L to cathepsin B activities, and vice versa, were determined by inclusion of parallel assays containing 5 μM

Downloaded from molpharm.aspetjournals.org by guest on December 1, 2012

MOL PHARM
MOLECULAR PHARMACOLOGY
aspet

CA-074, which inhibits cathepsin B. The only significant deviation from the published assay procedures was the use of 10 μM instead of 100 μM Ac-ED(Edans)KPILFFRLGK(Dabcyl)E-NH_2 in the cathepsin D assay. All cathepsin assays were scaled to work in 96-well plates. Cathepsin B specific activities are reported as nanomoles of AMC produced per minute per milligram of protein. Cathepsin D specific activities are reported as nanomoles of Edans fluorophore released per minute per milligram of protein.

Whole-cell lysates for cathepsin enzymatic assays were prepared by flooding cultures with 0.25 M sucrose, 25 mM MES, pH 6.5, 1 mM EDTA, and 0.1% Triton X-100. After ~1 min, cell lysate was transferred to a microcentrifuge tube, sonicated for 1 s, and centrifuged for 13,000*g* for 5 min. Supernatant fluids were aliquoted and stored at −80°C. The procedure described under "Western Blot Analyses" was used to prepare lysosomal extracts for subsequent analyses of cathepsin activities.

Results

NPe6 Loading of 1c1c7 and Tao Lysosomes. The amount of singlet oxygen generated in PDT protocols is influenced by both the concentration of photosensitizer present in cells and the light dose. Hence, meaningful comparisons of the susceptibilities of different cell lines to photosensitizers require knowledge of cellular photosensitizer levels after sensitization. Figure 1A depicts analyses of cell-associated NPe6 contents after a 1-h sensitization period. NPe6 loading was linear over the 11 to 66 μM range examined in both 1c1c7 and Tao cultures. Per-cell NPe6 contents were ~5 to 15% higher in Tao cultures at all concentrations examined. Similar results were obtained in two additional experiments, and per-cell NPe6 contents were identical in a fourth experiment. Hence, the NPe6 per cell contents of Tao cells were comparable with, if not slightly greater than, those of 1c1c7 cells. Maximal loading of either cell type with sensitizer occurred within 30 min of adding 33 μM NPe6 (Fig. 1B). Lengthening the sensitization period to 1 or 2 h had little effect on cell–associated NPe6 contents (Fig. 1B). Results similar to those reported in Fig. 1B were also obtained when either cell type was sensitized with 16 or 66 μM (J. J. Reiners, unpublished data). In subsequent studies, cultures were sensitized for 45 to 60 min with either 33 or 66 μM NPe6.

We recently demonstrated by microscopy that NPe6 fluorescence in 1c1c7 cells colocalized to a subset of organelles also labeled by LysoTracker Blue (Reiners et al., 2002). At issue is whether the NPe6 loading data reported in Fig. 1A correlate with the acidic organelle contents of the two cell lines. To address this issue, we loaded cultures with the lysosomotropic weak base acridine orange (AO), which fluoresces red in acidic environments, and quantitated fluorescence by flow cytometry. Figure 1, C and D, shows the overlays of such analyses for three different cultures of each cell line. Staining was very reproducible from culture to culture. In agreement with the NPe6 loading estimates, AO content was slightly higher (~10%) in Tao cells.

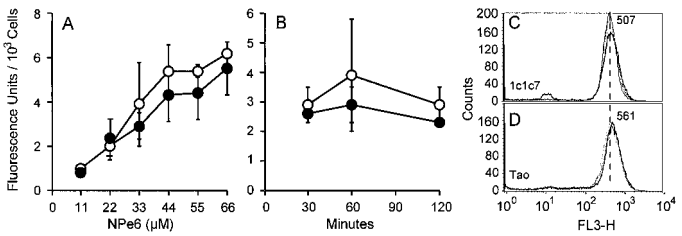

Fig. 1. NPe6 loading of 1c1c7 and Tao cultures. A, nearly confluent 1c1c7 (●) and Tao (○) cultures were loaded with various concentrations of NPe6 for 1 h before being processed for NPe6 determinations as described under *Materials and Methods*. B, cultures were loaded with 33 μM NPe6 for 30, 60, or 120 min before being harvested for analyses of NPe6 contents. Data represent means ± S.D. of analyses performed on four plates per treatment. Similar data were obtained in three additional independent experiments. C and D, FACS analyses of acridine orange staining of lysosomes in 1c1c7 (C) and Tao (D) cells. Data represent overlays of analyses performed on three cultures of each cell type. Value above peak represents mean of FL3-H mean values taken from the histograms of three culture dishes.

NPe6 Cytotoxicity. A colony formation assay was used to compare the sensitivities of 1c1c7 and Tao cultures with NPe6-mediated killing in a PDT protocol. A 1-h exposure to 33 or 66 μM NPe6, in the absence of irradiation, reduced Tao and 1c1c7 colony formation by ~12% and ~6%, respectively (Fig. 2). In the absence of NPe6, irradiation for 130 to 150 s did not affect the viability of either cell line (Fig. 2). However, NPe6-sensitized cultures were killed by subsequent irradia-

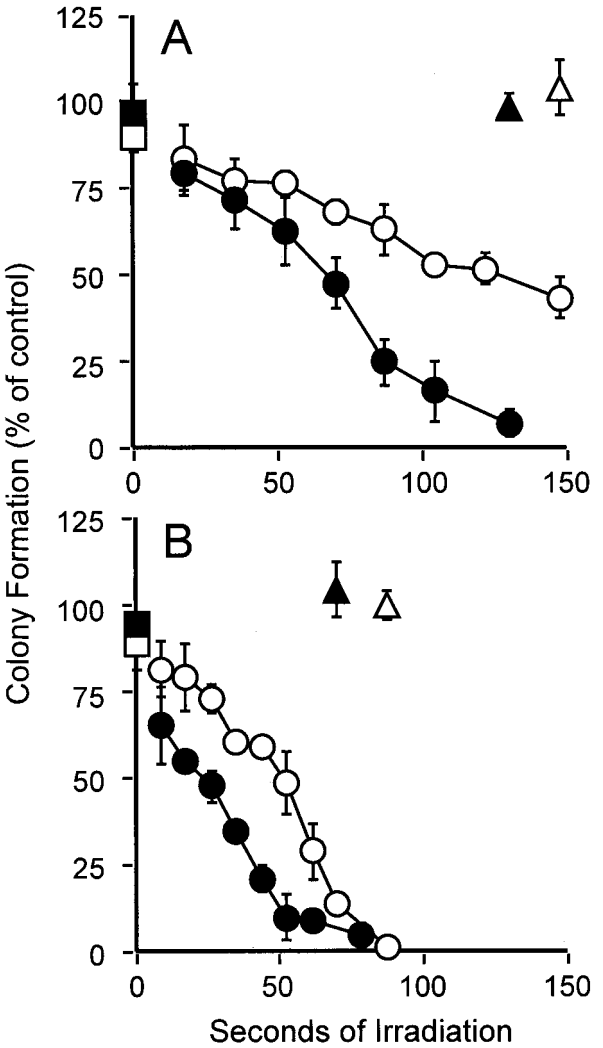

Fig. 2. NPe6 cytotoxicity as assessed in colony-forming assays. 1c1c7 (solid symbols) or Tao (open symbols) cells were plated at densities of 250 to 1600 cells per 60-mm dish ~20 h before a 1-h sensitization with either 33 μM NPe6 (A) or 66 μM NPe6 (B). After the indicated lengths of irradiation, cultures were returned to an incubator. Colonies were counted 8 to 10 days after irradiation. ■,□, NPe6 only; ▲,△, light only; ●,○, NPe6 + light. Data represent the means ± S.D. of three to four plates per treatment group. Similar survival curves were generated in three additional experiments with each concentration of sensitizer.

Downloaded from molpharm.aspetjournals.org by guest on December 1, 2012

MOL PHARM
MOLECULAR PHARMACOLOGY
aspet

tion in a light dose-dependent and NPe6 concentration-dependent manner (Fig. 2). 1c1c7 cultures sensitized with either 33 μM (Fig. 2A) or 66 μM (Fig. 2B) NPe6 were markedly more sensitive than Tao cultures at each light dose tested.

NPe6-Induced Lysosome Breakage. We recently reported that irradiation of NPe6-sensitized 1c1c7 cultures causes lysosomal damage and the loss of AO staining (Reiners et al., 2002). AO staining in nontreated 1c1c7 and Tao cultures was punctate and perinuclear (Fig. 3). Exposure to 140 s of light had little effect on the distribution or staining intensity of AO-labeled lysosomes. In cultures preloaded with 33 μM NPe6, AO staining remained perinuclear but was somewhat coalesced (Fig. 3). Irradiation of cultures preloaded with 33 μM NPe6 resulted in a light dose-dependent loss of AO staining. However, less AO staining was observed in 1c1c7 cultures, relative to Tao cultures, at every light dose analyzed. Staining was eliminated in 1c1c7 cultures irradiated for 140 s. In contrast, approximately 40% of the cells in Tao cultures exhibited strong punctuate AO staining (Fig. 3 and one additional experiment involving the analyses of ~100 cells). This percentage of Tao cells with detectable punctate AO staining after 140 s of irradiation is very similar to the percentage of cells that survived after similar treatment, as scored in colony formation assays (compare Figs. 2A and 3).

The differential sensitivities of 1c1c7 and Tao lysosomes to disruption in NPe6-PDT protocols were also seen when 66 μM NPe6 was used for sensitization (data not shown). At comparable light doses, less AO staining was consistently observed in 1c1c7 cultures. Whereas 50 s of irradiation was sufficient to eliminate AO staining in 1c1c7 cultures, a comparable effect in Tao cells required ~80 s of irradiation. Hence, although 1c1c7 and Tao cells contained similar amounts of NPe6, Tao lysosomes were more resistant to disruption after irradiation.

PDT-Induced Apoptosis in 1c1c7 and Tao Cultures. After irradiation, NPe6-sensitized 1c1c7 and Tao cultures underwent pronounced morphological changes indicative of apoptosis (Fig. 4). However, the rate at which cultures expressed apoptotic features differed for the two cell lines. This point is best documented by comparing cultures treated with PDT conditions causing comparable cell killing. For cultures sensitized with 66 μM NPe6, an LD_{50} for 1c1c7 and Tao cells required ~20 and ~50 s of irradiation, respectively (Fig. 2). Shrunken, blebbed cells were obvious in 1c1c7 cultures within 4 h of irradiation (Fig. 4C), whereas no apoptotic cells were observed in Tao cultures (Fig. 4F). Within 8 h of irradiation, with LD_{50} conditions, both cell types were undergoing apoptosis (Fig. 4, I and L). However, 1c1c7 cultures were much further along in the apoptotic process based upon the copious presence of apoptotic bodies. Similar results were obtained when cultures were irradiated using ~LD_{90} conditions (i.e., 50 s for 1c1c7 cultures and 75 s for Tao cultures). At 4 h after irradiation, multiple blebbed cells were clearly present in 1c1c7 cultures (Fig. 4E), whereas only an occasional blebbed cell was observed in Tao cultures (Fig. 4H). Within 8 h of irradiation, with LD_{90} conditions, both cultures were undergoing apoptosis. However, blebbing was most prominent in the 1c1c7 cultures (Fig. 4, K versus N).

Although both 1c1c7 and Tao cultures underwent morphological changes characteristic of apoptotic cells after PDT, we

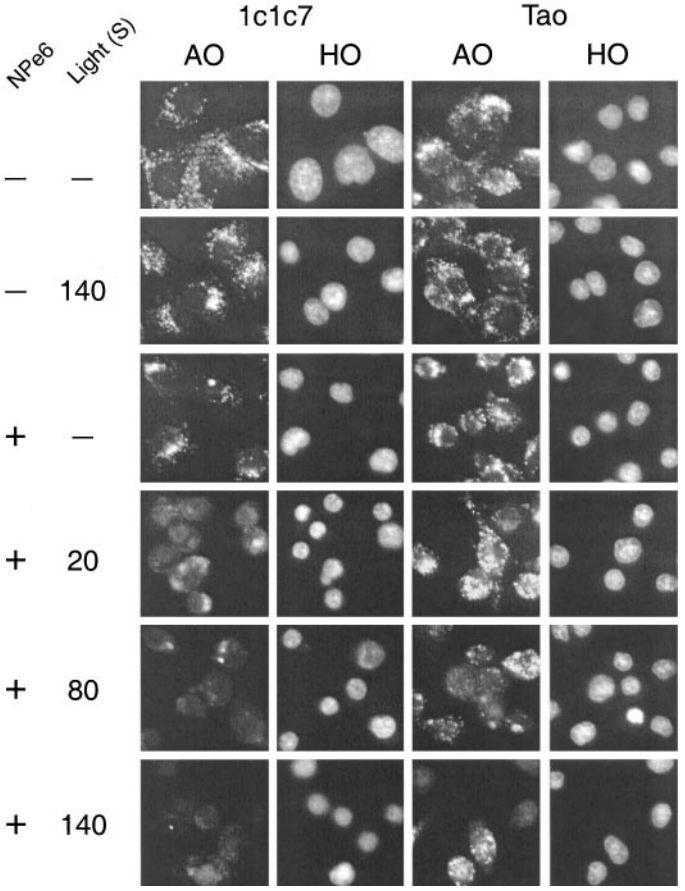

Fig. 3. Differential sensitivities of 1c1c7 and Tao lysosomes to NPe6-induced disruption in PDT protocols. 1c1c7 and Tao cultures grown on coverslips were loaded with 33 μM NPe6 for 45 min before being washed and irradiated for the indicated lengths of time. After 1 h, cultures were loaded with AO and HO33342 to visualize lysosomes and nuclei, respectively. Approximately 15 min later, coverslips were washed with PBS and used for fluorescence microscopy. Control cultures were treated with nothing, only NPe6, or only light. Figures are representative of two independent experiments.

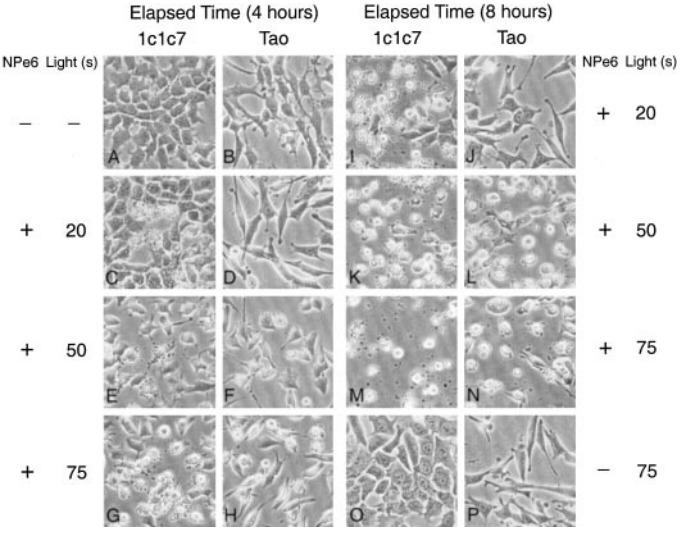

Fig. 4. Morphological changes after irradiation of NPe6-sensitized cultures. Cultures were loaded with 66 μM NPe6 for 45 min before being washed, refed, and irradiated for varied lengths of time. Control cultures were treated with nothing or irradiated for 75 s. Cultures were photographed either 4 or 8 h after irradiation.

Downloaded from molpharm.aspetjournals.org by guest on December 1, 2012

MOL PHARM
MOLECULAR PHARMACOLOGY
aspet

sought additional criteria to document the differential induction of apoptosis in the two cell lines. The flipping of phosphatidylserine from the inner to the outer plasma membrane occurs early in the apoptotic program and is often used as a specific marker of cells undergoing apoptosis. Flow cytometric analyses of FITC-conjugated annexin V binding to 1c1c7 and Tao cultures are presented in Fig. 5. In these studies, cells were counter-stained with propidium iodide (PI) to distinguish between apoptotic cells (annexin V^+/PI^-, upper left quadrant of the flow cytometry histograms) and oncotic cells that bind annexin V on the cytoplasmic side of the plasma membrane as a consequence of the membrane being permeable (annexin V^+/PI^+, upper right quadrant). It should be noted that late stage apoptotic cells often become PI-permeable and can be a component of the annexin V^+/PI^+ population.

Annexin V^+/PI^- 1c1c7 and Tao cells constituted only a small percentage of the culture population after no treatment, light-only treatment, or sensitization with 66 μM NPe6 (Fig. 5). However, there was a significant accumulation of annexin V^+/PI^- cells within 3 h of irradiating NPe6-sensitized 1c1c7 cultures for 50 s, and the percentage of annexin V^+/PI^- cells increased with passing time. In contrast, after similar treatments, Tao cultures exhibited markedly lower percentages of annexin V^+/PI^- cells at each of the three time points examined. However, the percentage of Tao cells scored as annexin V^+/PI^- could be enhanced by increasing the light dose by 1.5-fold (by irradiating for 75 s).

DEVDase activity is commonly used to monitor the collective activation of pro-caspases-3, -6, and -7. DEVDase activities were basically unaffected in nonsensitized 1c1c7 and Tao cultures after irradiation for ≤125 s (Fig. 6, A and B).

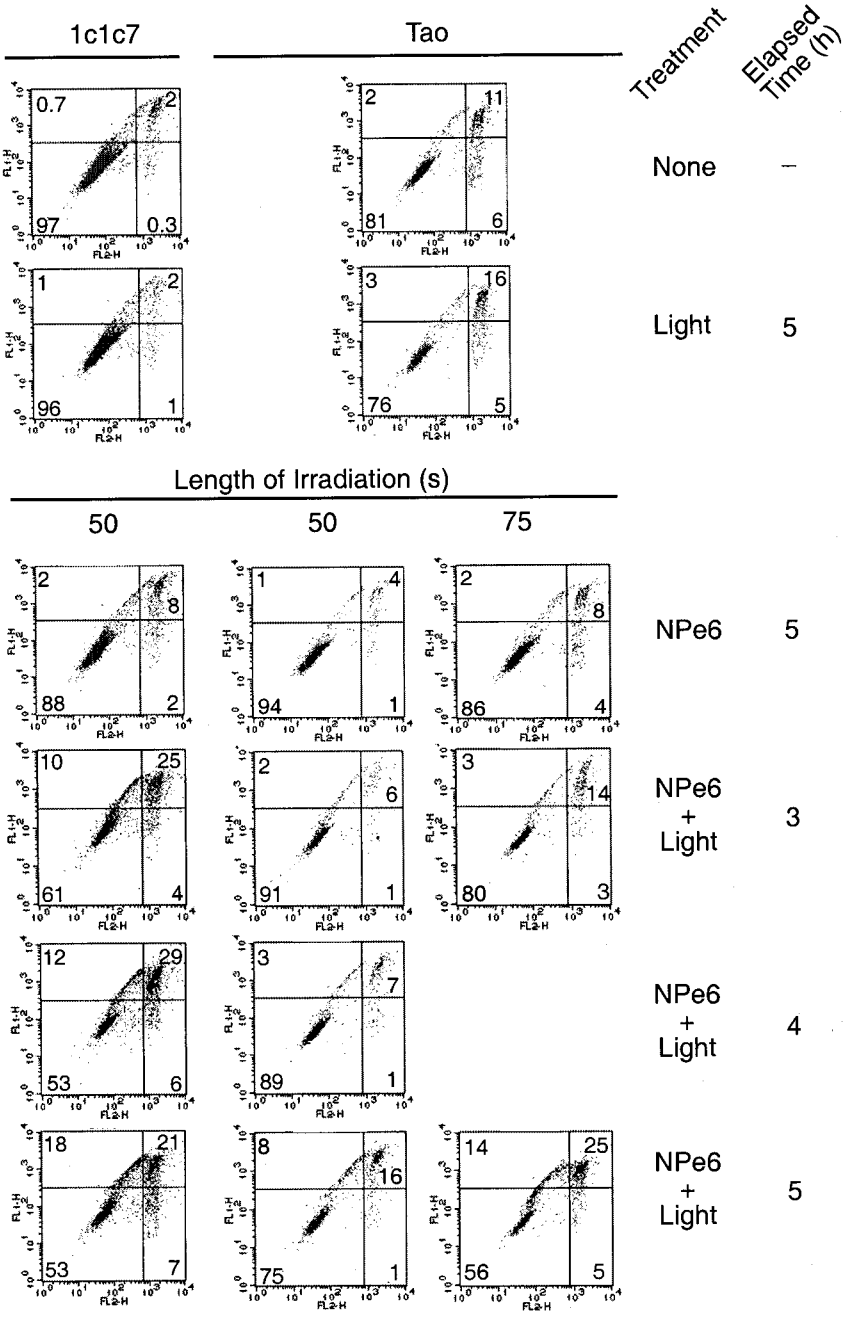

Fig. 5. Annexin V binding after irradiation of NPe6-sensitized cultures. Cultures of 1c1c7 and Tao cells were treated with nothing, 50 or 75 s of light, 66 μM NPe6, or NPe6 + light for various lengths of time (3–5 h) before being harvested for analyses of Annexin V and PI staining by flow cytometry. Annexin V and PI staining are represented on the *y*-axis (FL1-H) and *x*-axis (FL2-H), respectively. Analyses represent data collected on ~12,000 gated 1c1c7 cells and ~6000 gated Tao cells. Values in the quadrants represent the percentage of total gated cells. Similar data were obtained in a second independent experiment, which also included analyses performed with 33 μM NPe6, at the 3- and 5-h time points.

Downloaded from molpharm.aspetjournals.org by guest on December 1, 2012

MOL PHARM
MOLECULAR PHARMACOLOGY
aspet

Similarly, DEVDase activities were not elevated after exposure to just 33 μM NPe6 or 66 μM NPe6 (Fig. 6, C and D). However, dramatic increases in DEVDase activities occurred in both cell lines after the irradiation of NPe6-sensitized cultures. In both lines, with either concentration of sensitizer, the kinetics of DEVDase activation correlated with the length of irradiation so long as $<LD_{95}$ conditions were used in the PDT protocol. Thereafter, DEVDase-specific activities reached a maximum and could not be increased by lengthening the irradiation times. Increasing the sensitizer concentration from 33 μM to 66 μM decreased the amount of light required for maximal DEVDase activation in both cell lines.

At fixed light doses, with either concentration of sensitizer, Tao cultures consistently expressed lower DEVDase specific activities than 1c1c7 cells. The differences between the DEVDase specific activities of the two cell lines could be minimized if analyses were made between samples prepared from cultures having comparable survival/LD values. This minimization is consistent with the observation that Tao cultures needed to be irradiated longer than 1c1c7 cultures to accomplish similar killing and lysosome breakage. Nevertheless, maximum DEVDase-specific activities were not identical in the two cell lines. Maximum DEVDase-specific activities in 1c1c7 cells were consistently 5- to 8-fold higher (Fig. 6, C and D; three additional experiments).

Irradiation alone or exposure to NPe6 alone did not trigger the proteolytic cleavages of Bid, pro-caspase-9, or pro-caspase-3 in either 1c1c7 or Tao cells, as assessed by Western blot analyses (Fig. 7). However, PDT did cause a rapid activation of pro-caspase-9 in 1c1c7 cells, which preceded the activation of pro-caspase-3. The activation of pro-caspase-9 in 1c1c7 cells was paralleled/accompanied by the loss of Bid (Fig. 7A). In contrast, no caspase-9 or -3 cleavage products were detected in sensitized and irradiated Tao cells when comparable ECL exposure times were used for detection of immune complexes (data not shown). Pro-caspase-9 and -3 cleavage products could be detected in Tao cells if the ECL exposure times were significantly lengthened (Fig. 7B). Even then, however, the relative amounts of cleavage products were much lower than what was detected with 1c1c7 lysates. Bid cleavage in Tao cultures paralleled pro-caspase-9 activation. The kinetics of disappearance were considerably slower than that observed in 1c1c7 cultures.

CD95 and HA14–1 Induced Apoptosis. To determine whether the differential responses of 1c1c7 and Tao cultures to PDT reflected a general resistance of Tao cells to apoptosis, we compared the responses of the two cell lines to different classes of apoptotic inducers. HA14–1 activates the intrinsic apoptotic pathway via its ability to bind the hydrophobic cleft of anti-apoptotic Bcl-2 family members (Wang et al., 2000). Cotreatment of either 1c1c7 or Tao cells with HA14–1 resulted in a concentration-dependent induction of apoptosis. Neither the kinetics nor magnitude of induction of DEVDase activities was markedly different in either cell line (Fig. 8A). The Jo2 antibody activates the extrinsic apoptotic pathway via its ability to cross-link and activate the CD95 receptor. Coincubation of either cell line with cycloheximide and the Jo2 antibody resulted in apoptosis, as scored morphologically (data not presented) and by measurement of DEVDase activity (Fig. 8B). The kinetics and magnitude of DEVDase acti-

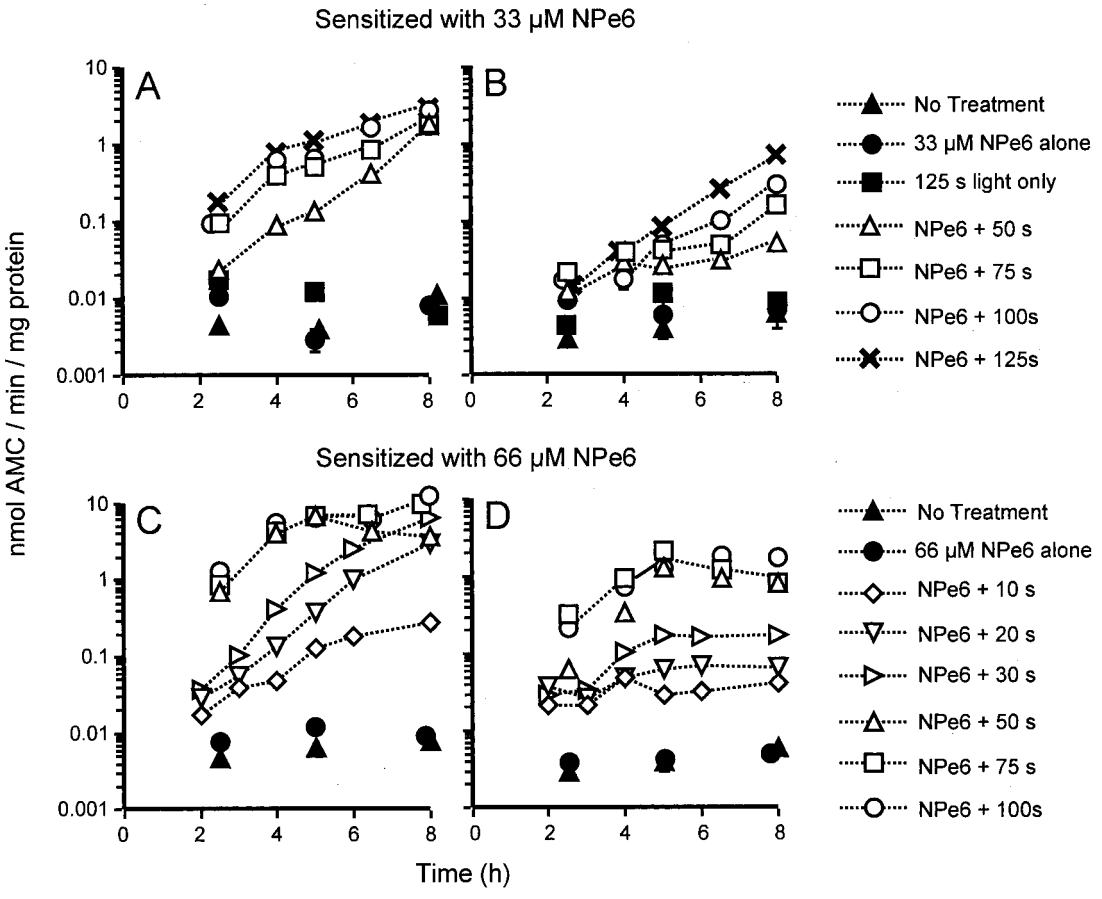

Fig. 6. Caspase activation after irradiation of NPe6-sensitized cultures. Cultures of 1c1c7 (A and C) and Tao (B and D) cells were loaded with either 33 μM (A and B) or 66 μM (C and D) NPe6 for 45 min before being washed, refed, and irradiated for various lengths of time. Control cultures were treated with nothing, treated only with NPe6, or irradiated for 125 s. The specifics of treatment are noted in the figure. Cultures were harvested at various times after irradiation for determination of DEVDase activities. Data represent means ± S.D. of triplicate analyses performed on the lysate prepared from a single plate. Error bars are hidden by symbols. Similar results were obtained in a second independent experiment.

Downloaded from molpharm.aspetjournals.org by guest on December 1, 2012

MOL PHARM
MOLECULAR PHARMACOLOGY
aspet

vation were virtually identical for the two cell lines. We previously reported that the kinetics and magnitude of DEVDase activation were identical for the two cell lines after exposure to apoptotic concentrations of staurosporine or doxorubicin (Reiners and Clift, 1999). Hence, the differential sensitivities of NPe6-sensitized 1c1c7 and Tao cultures to PDT do not reflect an inherent resistance of the Tao line to apoptosis.

Bid Cleavage by Lysosomal Extracts. We recently reported that extracts prepared from isolated 1c1c7 lysosomes contain an activity capable of cleaving Bid in vitro (Reiners et al., 2002). Figure 9A compares in vitro Bid cleavage mediated by extracts prepared from purified preparations of 1c1c7 and Tao lysosomes. The source of Bid in these studies was 1c1c7 cytosolic supernatant fractions created by centrifugation at 100,000*g*. Whereas lysosomal extracts from 1c1c7 cells effectively cleaved Bid, less cleavage product was observed in reactions employing extracts from Tao lysosomes.

The cytosols of many cell types contain potent lysosomal protease inhibitors (for review, see Shridhar et al., 2000). To circumvent possible complications by cytosolic inhibitors, we used a second assay that substituted recombinant murine Bid for the Bid present in cytosolic preparations. Analyses of the abilities of lysosomal extracts to cleave recombinant Bid in the absence of any cytosol are presented in Fig. 9B. The extent of Bid cleavage varied directly with the amount of lysosomal extract from either cell line. However, more cleavage product was generated with 1c1c7 lysosomal extracts at each of the three protein concentrations tested [147 ± 5% of Tao content, Fig. 9B and 2 additional experiments ($p < 0.05$)].

Cathepsins in 1c1c7 and Tao Cells. Several studies have suggested that cathepsins B and D contribute to the initiation and development of the apoptotic program (Roberg et al., 1999; Guicciardi et al., 2000; Foghsgaard et al., 2001). Cathepsin B specific activities in 1c1c7 and Tao whole-cell lysates and purified endosome/lysosome lysates differed considerably from one another (Fig. 10A). Specifically, Tao cells

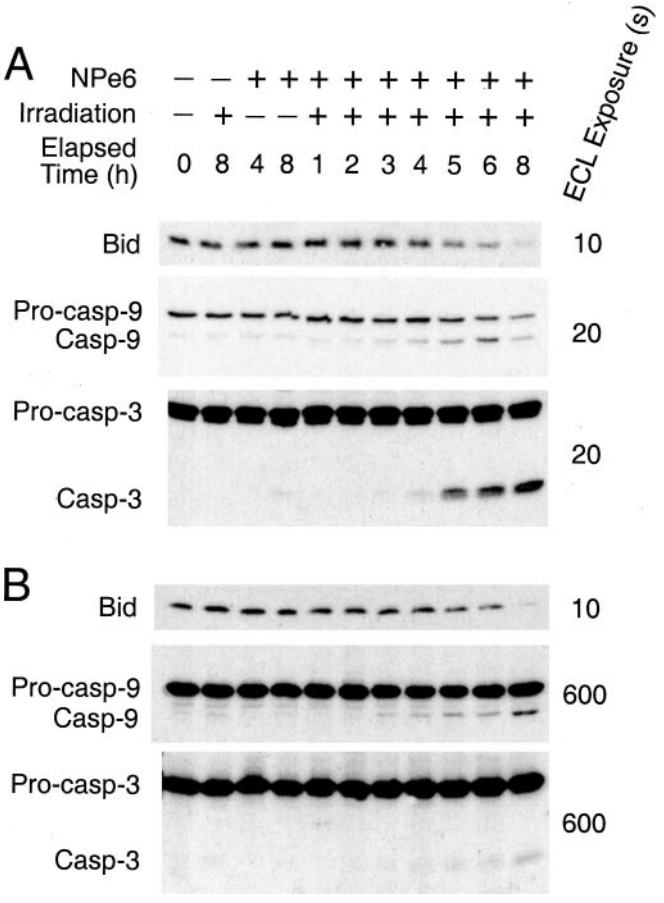

Fig. 7. Bid, pro-caspase-9, and pro-caspase-3 cleavage after irradiation of NPe6-sensitized cultures. Cultures of 1c1c7 (A) or Tao (B) cells were loaded with 66 μM NPe6 for 45 min before being washed, refed, and irradiated for 50 s (1c1c7) or 80 s (Tao). Control cultures were treated with nothing, only NPe6, or only light. Lysates were prepared 1 to 8 h after irradiation for subsequent Western blot analyses. Analyses of individual proteins from Tao and 1c1c7 cultures were performed on the same blots, at the same time, using a common reagent solution. Note that the ECL exposure times are very different for the Tao and 1c1c7 caspase-3 and -9 samples. Similar results were obtained in a second independent experiment.

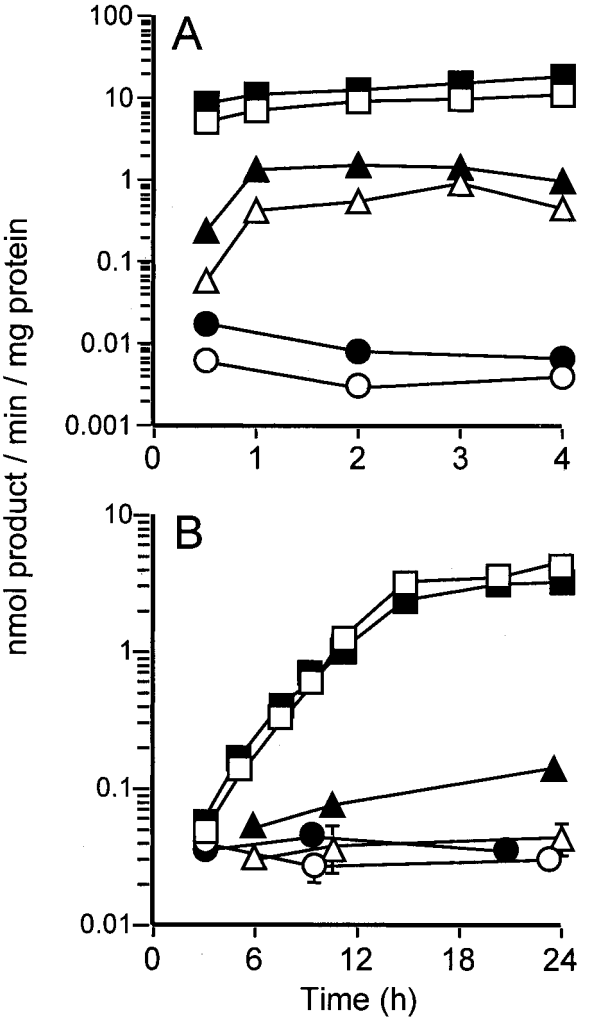

Fig. 8. Activation of the extrinsic and intrinsic apoptotic pathways. A, cultures of Tao (closed symbols) and 1c1c7 (open symbols) cells were treated with nothing (●,○), 15 μM HA14–1 (▲,△), or 25 μM HA14–1 (■,□) for various lengths of time before being harvested for DEVDase assays. B, cultures of Tao (closed symbols) and 1c1c7 (open symbols) cells were treated with nothing (●,○), 1 μg/ml CHX (▲,△), or 1 μg/ml CHX + 3 μg/ml Jo2 antibody (■,□). Cultures were incubated with CHX for 30 min before the addition of the Jo2 antibody. Cultures were harvested at indicated times for analyses of DEVDase activities. Results similar to those reported in A and B were obtained in a second independent experiment.

Downloaded from molpharm.aspetjournals.org by guest on December 1, 2012

had ~50% and ~35% of the whole cell and endosomal/lysosomal cathepsin B activities measured in 1c1c7 cultures. Tao cultures also contained less cathepsin D than 1c1c7 cultures. Cathepsin D-specific activities in lysates prepared from Tao cells and endosome/lysosome preparations were ~80% and ~55% of the values measured in 1c1c7 cells (Fig. 10A). Western blot analyses of whole-cell lysates suggested that Tao cells contained slightly less cathepsin B and D than 1c1c7 cells (Fig. 10, B and C). However, the differences were not statistically significant. In contrast, Tao lysosomal cathepsin B and D contents were only 35% and 25%, respectively, of 1c1c7 lysosomal contents (Fig. 10, B and C).

The 1c1c7/Tao cell pair is often used to assess the involvement of the AhR in biological processes. To determine whether the AhR might modulate lysosomal protease contents, we surveyed cathepsin B and D contents in a variant of the 1c1c7 line (WARV cells), having reduced AhR levels because of the stable expression of antisense AhR (Fig. 10D) and in a variant of the Tao cell line (TAHR) that was stably transfected with an AhR sense vector (Fig. 10D). Data generated with WARV and TAHR cells were compared with WCMV and TCMV cells, respectively. The latter two lines are variants of the 1c1c7 and the Tao lines that had been stably transfected with an empty expression vector (Fig. 10D). Whole-cell extracts of WARV versus WCMV cells and TAHR versus TCMV cells contained similar amounts of cathepsins B and D (Fig. 10, B and C). However, the endosomal/lysosomal contents of both cathepsins were markedly greater in the AhR-containing members (WCMV and TAHR cells) of the two stably transfected cell pairs.

NPe6 Loading of TAHR and TCMV Lysosomes. If the differential sensitivities of NPe6-sensitized 1c1c7 and Tao cultures to PDT were a consequence of AhR-mediated processes, it follows that the AhR-containing TAHR cell line should be more sensitive to NPe6 PDT than TCMV cells, its cognate AhR-deficient partner. Loading studies showed that TCMV cells contained more NPe6 than TAHR cells at each concentration of sensitizer tested (Fig. 11A). This difference qualitatively correlated with the lysosomal loading capacities of the two cell lines (Fig. 11, B and C). Flow cytometric analyses of AO fluorescence indicated that the lysosomal loading capacity of TAHR cells was ~65% of TCMV cells.

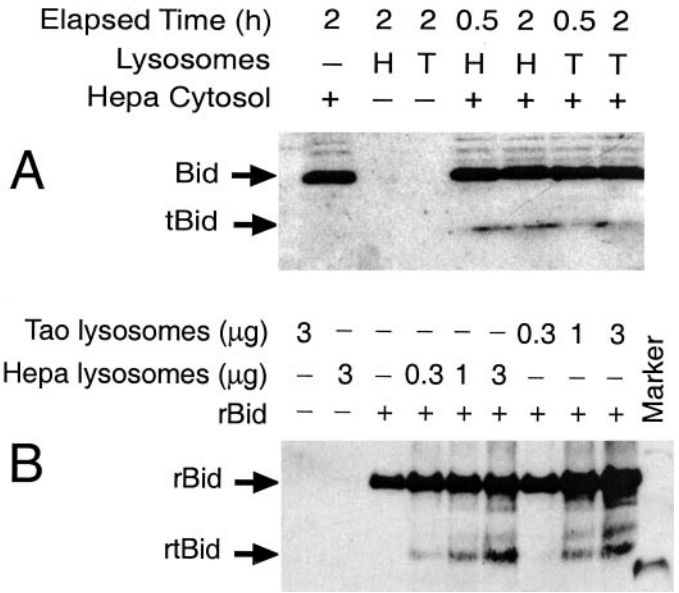

Fig. 9. In vitro cleavage of Bid by lysosomal extracts prepared from Hepa 1c1c7 and Tao cells. A, extracts of purified lysosomes (2 μg) isolated from Hepa (H) or Tao (T) cells were incubated with 10 μg of Hepa cytosol. After 0.5 or 2 h of incubation, the samples were harvested for Western blot analyses of Bid and tBid. Similar results were obtained in six additional experiments. B, recombinant murine Bid (40 ng) was incubated with varied amounts of Hepa 1c1c7 or Tao lysosomal extracts for 15 min before being processed for Western blot analyses of Bid. Similar results were obtained in two additional experiments.

PDT-Induced Apoptosis in TAHR and TCMV Cells. In initial studies, TAHR and TCMV cultures were sensitized for 1 h with 66 μM NPe6, and then irradiated for either 20 s (Fig. 12A) or 50 s (Fig. 12B). Time-dependent increases in DEVDase activities were noted in both cell lines after irradiation. DEVDase activities increased faster, and ultimately reached higher levels (~10-fold), in the TAHR line after 20 s of irradiation (Fig. 12A). The morphologies of TAHR cells indicated that a considerable portion of the culture was undergoing apoptosis. In contrast, only an occasional apoptotic cell was observed in TCMV cultures (J. J. Reiners, unpublished data). In contrast, after 50 s of irradiation, the kinetics and magnitudes of DEVDase activation were quite similar in the two cell lines (~2-fold difference in magnitude, Fig. 12B). This narrowing of the difference is similar to what was observed in the 1c1c7/Tao cell pair after irradiation with increased light doses (Fig. 6).

The loading studies reported in Fig. 11A suggest that TCMV cultures contain ~2× the NPe6 content of TAHR cells, when sensitized with 66 μM NPe6. Because the amount of singlet oxygen produced after irradiation is proportional to cellular NPe6 content, we attempted to equalize NPe6 loading by sensitizing TAHR and TCMV cultures with 66 and 33 μM NPe6, respectively (see Fig. 11A). A preferential activation of DEVDase occurred in the TAHR cell line after irradiation for 40 s (~4-fold; Fig. 12C). Analyses of pro-caspase-9 and -3 cleavage products emphasized the differential responses of the two cell lines to PDT (Fig. 12D). In the TAHR line, there were obvious time-dependent declines in pro-caspase-9 and -3 contents that were accompanied by the appearance of the processed/active forms of the caspases. In marked contrast, there were neither comparable losses of the two pro-caspases in the TCMV cell line nor significant accumulations of the active cleavage products (Fig. 12D).

Discussion

In the current study, we demonstrate that Tao cells, an AhR-deficient variant of the 1c1c7 cell line, are markedly more resistant than the parental line to the lysosomal photosensitizer NPe6 in PDT protocols. NPe6 preferentially accumulates in lysosomes and causes their destruction after irradiation via the production of singlet oxygen (Reiners et al., 2002). Loading studies indicated that the sensitivities of the two cell lines to PDT were not a consequence of differences in NPe6 contents after sensitization. Instead, cell survival in PDT protocols correlated with lysosome breakage. With either of the two NPe6 concentrations used for sensitization, at fixed light doses, less lysosomal damage occurred in Tao cells. To achieve comparable lysosomal damage, and cell killing, the Tao line had to be irradiated for longer periods than the 1c1c7 line. However, even when PDT conditions were adjusted to achieve comparable killing, Tao cul-

MOL PHARM
MOLECULAR PHARMACOLOGY
aspet
Downloaded from molpharm.aspetjournals.org by guest on December 1, 2012

MOL PHARM
MOLECULAR PHARMACOLOGY
aspet

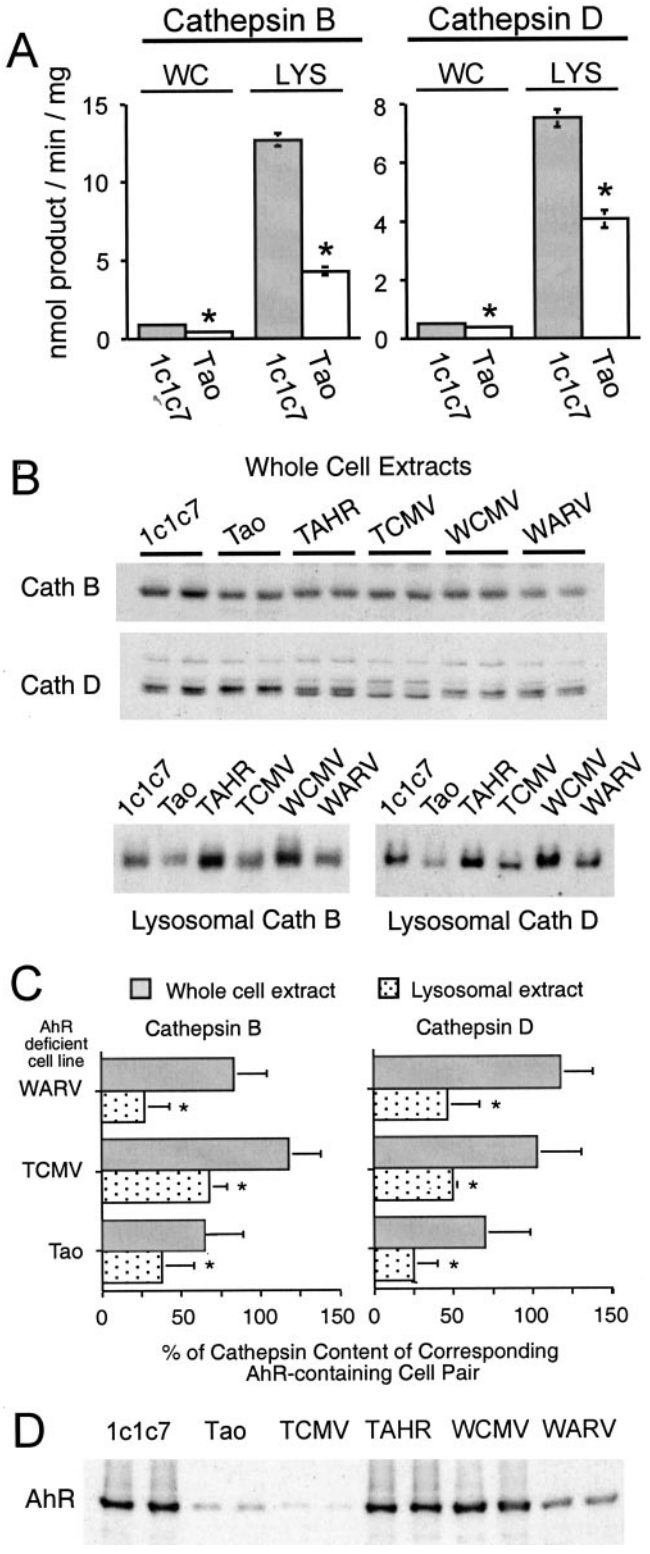

Fig. 10. AhR and cathepsin B and D contents of cells of 1c1c7 lineage. A, lysates of whole cells (WC) or isolated lysosomes/endosomes (LYS) from 1c1c7 and Tao cells were used for analyses of cathepsin B and D activities. Data represent means ± S.D. of three samples. *, statistically less than corresponding 1c1c7 sample, $p \leq 0.05$ by Student's t test. Similar data were obtained in a second independent experiment. B, Western blot analyses of cathepsins B and D in whole-cell and lysosomal preparations of 1c1c7/Tao variant cell lines. Gel lanes were loaded with 25 μg of whole-cell lysate and 2 or 4 μg of lysosomal extract for analyses of cathepsins B and D, respectively. Each lane in the whole cell extract blots represents a different culture dish. Each lysosomal protein lane represents a lysosomal preparation generated from 15 to 20 100-mm culture dishes. C, quantitative analyses of Western blot analyses of cathepsins B and D in AhR-containing and -deficient cell lines. The data represent analyses of four to five whole cell lysate preparations, and three to four lysosomal preparations, for each cell type. Data are presented as percentage of the cathepsin content of the AhR-containing pair for the pairs: 1c1c7 versus Tao, TAHR versus TCMV, and WCMV versus WARV (AhR-containing cell line noted first in the pairings). Statistical analyses were performed on band intensities before transformation to percentage of AhR-containing cell pair. *, statistically less than the cathepsin content of the corresponding cell pair, $p \leq 0.05$ by paired Student's t test. D, Western blot analyses of AhR contents in lysates of 1c1c7/Tao variant cells. Gel lanes were loaded with 20 μg of whole cell lysates.

tures developed apoptotic morphological features much more slowly than 1c1c7 cultures. This delay corresponded to reduced levels of activated initiator (i.e., caspase-9) and executioner (i.e., caspase-3) proteases in Tao cultures.

Our observation that the lysosomes of different cell lines differ in their susceptibility to breakage by oxidants/cytotoxic agents is not unique. Similar findings have been reported when TNFα or oxidants other than NPe6 were used as the cytotoxic agents (Nilsson et al., 1997; Werneburg et al., 2002). Nilsson et al., (1997) have also shown that individual lysosomes within a single cell can differ in their susceptibilities to oxidant/detergent-induced disruption. Studies with iron chelators suggest that oxidant-induced lysosomal rupture is strongly influenced by lysosomal iron content (Persson et al., 2003). Wild-type p53 contents may also influence lysosome stability (Yuan et al., 2002). Recent studies have also implicated lysosomal cathepsin B in the regulation of lysosome fragility. Specifically, whereas TNFα treatment of cultured primary rat hepatocytes caused a release of lysosomal proteases, a comparable release did not occur in hepatocytes derived from cathepsin B-null mice (Werneburg et al., 2002). Furthermore, lysosomes prepared from cathepsin B null mice were less sensitive in vitro to the permeabilizing effects of sphingosine (Werneburg et al., 2002). Western blot and enzymatic analyses clearly indicated that, relative to the parental 1c1c7 line, Tao cells had reduced cathepsin B contents. However, we have found that pharmacological inhibition of cathepsin B activity in 1c1c7 cells does not suppress Bid cleavage, activation of DEVDase, or the development of apoptosis after PDT (LD_{95} conditions, Reiners et al., 2002; J. A. Caruso, unpublished data). Hence, it is unlikely that the differences noted in the current study are related to the lysosomal contents of cathepsin B.

We reported previously that the release of cytochrome c and activation of pro-caspase-9 in NPe6-sensitized 1c1c7 cultures after PDT occurs without the loss of mitochondrial membrane potential ($\Delta\Psi_m$) and is preceded/accompanied by the cleavage of Bid (Reiners et al., 2002). The proteolytic cleavage of Bid to tBid facilitates the ability of this proapoptotic protein to function in conjunction with Bak or Bax to trigger cytochrome c release (Korsmeyer et al., 2000; Wei et al., 2000). Because lysosomes contain an activity capable of cleaving Bid (Stoka et al., 2001; Reiners et al., 2002; this study), the finding that Tao lysosomes contain less Bid cleavage activity could be relevant to why Tao cells developed a delayed and muted apoptotic response after PDT. However, it should be noted that studies employing Bid-null cells suggest that lysosomal proteases can initiate the intrinsic apoptotic pathway independent of Bid (Boya et al., 2003). In such studies, a drop in $\Delta\Psi_m$ preceded the release of cytochrome c

Downloaded from molpharm.aspetjournals.org by guest on December 1, 2012

MOL PHARM
MOLECULAR PHARMACOLOGY
aspet

and activation of pro-caspase-3. Although a non-Bid pathway may contribute to the initiation of apoptosis in NPe6-sensitized 1c1c7/Tao cells after PDT, we have never detected a loss of $\Delta\Psi_m$ in 1c1c7 or Tao cultures in a NPe6-PDT protocol until the cells were very advanced in the apoptotic program (Reiners et al., 2002; J. J. Reiners, unpublished data).

In addition to the Bid-cleavage activity, Tao lysosomes/endosomes also had cathepsin B and D activities/contents lower than their 1c1c7 counterparts. A previous NPe6-PDT study suggested that neither of these two cathepsins was responsible for Bid cleavage in 1c1c7 cultures (Reiners et al., 2002). Activity measurements have also demonstrated that β-hexosaminidase and cathepsin L activities are reduced in Tao lysosome/endosome preparations (J. A. Caruso, unpublished data). Hence, the lysosomes/endosomes of Tao cells seem to be deficient in several proteases/hydrolases. Because our Western blot analyses were normalized on the basis of protein, it follows that the observed reductions reflect offsetting increases in other lysosomal/endosomal proteins. SDS PAGE analyses of purified lysosomes have consistently shown the presence of several polypeptides that are unique or more abundant in Tao preparations (J. A. Caruso, unpublished data). To a degree, Tao cells are analogous to fibroblasts (I cells) derived from patients suffering from mucolipidosis II or inclusion-cell disease. The lysosomes of I cells are deficient in many lysosomal proteases because of a defect that affects the processing and trafficking of newly synthesized proteases/hydrolases through the trans-Golgi network (McDowell and Gahl, 1997). I cell lysosomes are functionally inefficient and accumulate undegraded material (McDowell and Gahl, 1997). Similar to the Tao/1c1c7 cell pair, the apoptotic program in I cells develops slower, and is muted, relative to wild-type fibroblasts after exposure to agents causing lysosomal disruption (Terman et al., 2002).

The 1c1c7/Tao pair is commonly used to assess AhR involvement in mediating biological processes. Because the Tao line was derived from 1c1c7 cells by chemical mutagenesis, it is conceivable that the noted differences in lysosomal protease contents may be independent of the AhR. However, analyses of 1c1c7 and Tao variant lines in which AhR contents were decreased or restored by molecular approaches also showed that cathepsin B and D contents were reduced in the lysosomes of AhR-deficient cells. Surprisingly, AhR content did not markedly alter whole-cell cathepsin B and D contents. Collectively, these findings suggest that AhR content may affect the processing/trafficking of some newly synthesized proteins that are normally earmarked for delivery to the endosome/lysosome. To the best of our knowledge, the current studies are the first to suggest that the AhR may regulate such processes.

The current studies may provide a mechanistic explanation for the reported resistance of Tao, TCMV, and WARV

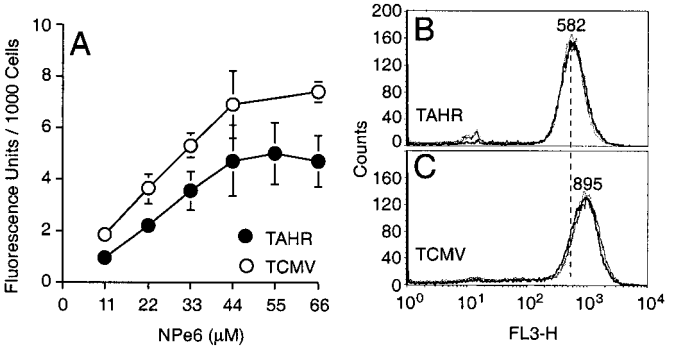

Fig. 11. NPe6 loading of TAHR and TCMV cultures. A, nearly confluent TAHR (●) and TCMV (○) cultures were loaded with various concentrations of NPe6 for 1 h before being processed for NPe6 determinations as described under *Materials and Methods*. B and C, FACS analyses of acridine orange staining of lysosomes in TAHR (B) and TCMV (C) cells. Data represent overlays of analyses performed on three cultures of each cell type. Value above peak represents mean of FL3-H mean values taken from the histograms of three culture dishes.

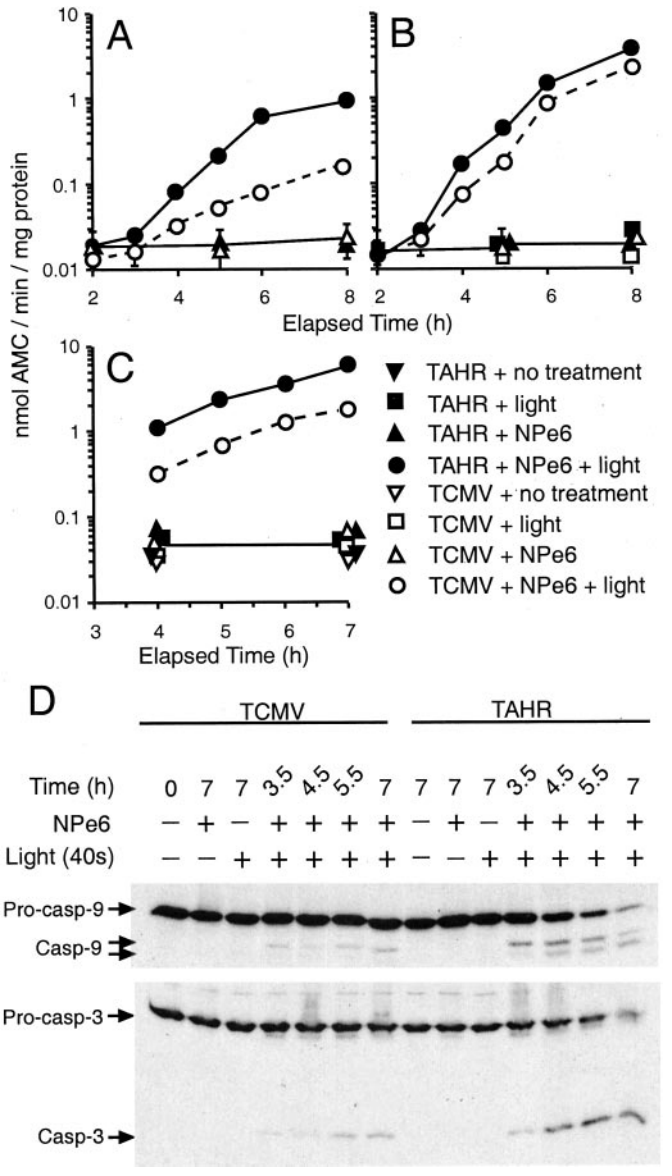

Fig. 12. Caspase activation after irradiation of NPe6-sensitized TAHR and TCMV cultures. A and B, cultures of TAHR (●) and TCMV (○) were treated with nothing, 66 μM NPe6, light, or NPe6 + light for various lengths of time before being harvested for analyses of DEVDase activity. Lengths of irradiation in A and B were 20 and 50 s, respectively. C, cultures of TAHR (●) and TCMV (○) were treated with nothing, NPe6, 40 s of light, or NPe6 + light for various lengths of time before being harvested for analyses of DEVDase activity. TAHR and TCMV cultures were sensitized with 66 and 33 μM NPe6, respectively. Data in A to C represent means ± S.D. of triplicate analyses performed on a single plate. D, cultures of TAHR and TCMV cells were treated as described in C for various lengths of time before preparation of lysates for subsequent Western blot analyses. Analyses were performed on 25 μg of lysate.

Downloaded from molpharm.aspetjournals.org by guest on December 1, 2012

cells, relative to their AhR-containing counterparts, to the proapoptotic effects of C_2-ceramide (Reiners and Clift, 1999). Specifically, ceramidase converts ceramide to sphingosine. The latter sphingolipid causes in vitro lysosomal permabilization when added directly to lysosome/endosome preparations (Kagedal et al., 2001; Werneburg et al., 2002) and has been implicated in the in vivo permeabilization of lysosomes (Kagedal et al., 2001; Werneburg et al., 2002). We have found that C_2-ceramide-treated 1c1c7 cultures release lysosomal proteases and cleave Bid with kinetics that precede/accompany cytochrome *c* release (J. A. Caruso and J. J. Reiners, unpublished data). It is conceivable that the AhR-deficient variant lines are resistant to the pro-apoptotic effects of C_2-ceramide because they contain insufficient amounts of lysosomal proteases needed to optimally initiate the apoptotic pathway. Then again, the lysosomes of AhR-deficient cells may be more resistant to the permeabilizing effects of sphingosine.

The current studies may also provide an explanation for some of the phenotypic characteristics of AhR knockout mice. Specifically, AhR-null mice develop a cardiomyopathy with many features identical to the cardiomyopathy occurring in cathepsin L-null mice (Fernandez-Salguero et al., 1997; Stypmann et al., 2002). AhR- and cathepsin L-null mice also develop similar, but not identical, cutaneous lesions involving the hair follicle (Fernandez-Salguero et al., 1997; Tobin et al., 2002). Preliminary analyses of Tao and 1c1c7 lysosomes/endosomes indicate that Tao cells have ~40% of the cathepsin L activity of 1c1c7 cells. Analyses of lysosomes isolated from wild-type C57BL/6 and AhR-null mice should shed light on whether the observations made with cells of the 1c1c7 lineage are relevant to the phenotypic similarities of AhR-null and cathepsin L-null mice.

Various cytotoxicants induce the release/translocation of lysosomal proteases into the cytosol. Examples of such agents include reactive oxygen species and generators of reactive oxygen species (Roberg et al., 1999; Antunes et al., 2001; Reiners et al., 2002; Boya et al., 2003), *O*-methyl-serine dodecylamide hydrochloride (Li et al., 2000), α-tocopheryl succinate (Neuzil et al., 2002), tumor necrosis factor α (Guicciardi et al., 2000; Foghsgaard et al., 2001; Werneburg et al., 2002), sphingosine (Kagedal et al., 2001), and the quinolone antibiotic ciprofloxacin (Boya et al., 2003). The release of lysosomal proteases into the cytosol can result in cell death with features of necrosis, apoptosis, or a combination of the two. Cell lines of the 1c1c7 lineage should be useful in determining the parameters that regulate lysosome fragility and the development of necrotic/apoptotic features after lysosomal protease release. The cell lines should also be useful in addressing the issues of whether and how the AhR regulates these processes.

References

Antunes F, Cadenas E, and Brunk UT (2001) Apoptosis induced by exposure to a low steady-state concentration of hydrogen peroxide is a consequence of lysosomal rupture. *Biochem J* **356:**549–555.

Boya P, Andreau K, Poncet D, Zamzami N, Perfettini J-L, Metivier D, Ojcius DM, Jäättelä M, and Kroemer G (2003) Lysosomal membrane permeabilization induces cell death in mitochondrion-dependent fashion. *J Exp Med* **197:**1323–1334.

Colell A, Morales A, Fernandez-Checa JC, and Garcia-Ruiz C (2002) Ceramide generated by acidic sphingomyelinase contributes to tumor necrosis factor-α-mediated apoptosis in human colon HT-29 cells through glycosphingolipids formation. *FEBS Lett* **526:**135–141.

Dougherty TJ, Gomer CJ, Henderson BW, Jori G, Kessel D, Korbelik M, Moan J, and Peng Q (1998) Photodynamic therapy. *J Natl Cancer Inst* **90:**889–905.

Dong L, Ma Q, and Whitlock JP Jr (1997) Down-regulation of major histocompatibility complex Q1b gene expression by 2,3,7,8-tetrachlorodibenzo-*p*-dioxin. *J Biol Chem* **272:**29614–29619.

Elizondo G, Fernandez-Salguero P, Sheikh MS, Kim GY, Fornace AJ, Lee KS, and Gonzalez FJ (2000) Altered cell cycle control at the G_2/M phases in aryl hydrocarbon receptor-null embryo fibroblast. *Mol Pharmacol* **57:**1056–1063.

Fernandez-Salguero PM, Ward JM, Sundberg JP, and Gonzalez FJ (1997) Lesions of aryl-hydrocarbon receptor-deficient mice. *Vet Pathol* **34:**605–614.

Foghsgaard L, Wissing D, Mauch D, Lademann U, Bastholm L, Boes M, Elling F, Leist M, and Jäättelä M (2001) Cathepsin B acts as a dominant execution protease in tumor cell apoptosis induced by tumor necrosis factor. *J Cell Biol* **153:**999–1009.

Gonzalez FJ and Fernandez-Salguero P (1998) The aryl hydrocarbon receptor: Studies using the AHR-null mice. *Drug Metab Dispos* **26:**1194–1198.

Gu YZ, Hogenesch JB, and Bradfield CA (2000) The PAS superfamily: sensors of environmental and developmental signals. *Annu Rev Pharmacol Toxicol* **40:**519–561.

Guicciardi ME, Deussing J, Miyoshi H, Bronk SF, Svingen PA, Peters C, Kaufmann SH, and Gores GJ (2000) Cathepsin B contributes to TNF-α-mediated hepatocyte apoptosis by promoting mitochondrial release of cytochrome c. *J Clin Invest* **106:**1127–1137.

Guo M, Mathieu PA, Linebaugh B, Sloane BF, and Reiners JJ Jr (2002) Phorbol ester activation of a proteolytic cascade capable of activating latent transforming growth factor-β. *J Biol Chem* **277:**14829–14837.

Hahn ME (1998) The Ah receptor: a comparative perspective. *Comp Biochem Phys* **121:**23–53.

Hankinson O (1995) The aryl hydrocarbon receptor complex. *Annu Rev Pharmacol Toxicol* **35:**307–340.

Kagedal K, Zhao M, Svensson I, and Brunk UT (2001) Sphingosine-induced apoptosis is dependent on lysosomal proteases. *Biochem J* **359:**335–343.

Kessel D, Luo Y, Mathieu P, and Reiners JJ Jr (2000) Determinants of the apoptotic response to lysosomal photodamage. *Photochem Photobiol* **71:**196–200.

Korsmeyer SJ, Wei MC, Saito M, Weiler S, Oh KJ, and Schlesinger PH (2000) Proapoptotic cascade activated BID, which oligomerizes BAK or BAX into pores that result in the release of cytochrome c. *Cell Death Differ* **7:**1166–1173.

Li W, Yuan X, Nordgren G, Dalen H, Dubowchik GM, Firestone RA, and Brunk UT (2000) Induction of cell death by the lysosomotropic detergent MSDH. *FEBS Lett* **470:**35–39.

Luberto C, Hassler DF, Signorelli P, Okamoto Y, Sawai H, Boros E, Hazen-Martin DJ, Obeid LM, Hannun YA, and Smith GK (2002) Inhibition of tumor necrosis factor-induced cell death in MCF7 by a novel inhibitor of neutral sphingomyelinase. *J Biol Chem* **277:**41128–41139.

Ma Q and Whitlock JP Jr (1996) The aromatic hydrocarbon receptor modulates the Hepa 1c1c7 cell cycle and differentiated state independently of dioxin. *Mol Cell Biol* **16:**2144–2150.

McDowell G and Gahl WA (1997) Inherited disorders of glycoprotein synthesis: Cell biological insights. *Proc Soc Exp Biol Med* **215:**145–157.

Nilsson E, Ghassemifar R, and Brunk UT (1997) Lysosomal heterogeneity between and within cells with respect to resistance against oxidative stress. *Histochem J* **29:**857–865.

Neuzil J, Zhao M, Ostermann G, Sticha M, Gellert N, Weber C, Eaton JW, and Brunk UT (2002) Alpha-tocopheryl succinate, an agent with in vivo anti-tumor activity, induces apoptosis by causing lysosomal instability. *Biochem J* **362:**709–715.

Persson HL, Yu Z, Tirosh O, Eaton JW, and Brunk UT (2003) Prevention of oxidant-induced cell death by lysosomotropic iron chelators. *Free Radic Biol Med* **34:**1295–1305.

Reiners JJ Jr, Caruso JA, Mathieu P, Chelladurai B, Yin X-M, and Kessel D (2002) Release of cytochrome c and activation of pro-caspase-9 following lysosomal photodamage involves bid cleavage. *Cell Death Differ* **9:**934–944.

Reiners JJ Jr and Clift RE (1999) Aryl hydrocarbon receptor regulation of ceramide-induced apoptosis in murine hepatoma 1c1c7 cells. *J Biol Chem* **274:**2502–2510.

Roberg K, Johansson U, and Öllinger K (1999) Lysosomal release of cathepsin D precedes relocation of cytochrome c and loss of mitochondrial transmembrane potential during apoptosis induced by oxidative stress. *Free Rad Biol Med* **27:**1228–1237.

Ségui B, Cuvillier O, Adam-Klages S, Garcia V, Malagarie-Cazenave S, Lévêque S, Caspar-Bauguil S, Coudert J, Salvayre R, Krönke M, et al. (2001) Involvement of FAN in TNF-induced apoptosis. *J Clin Investig* **108:**143–151.

Shridhar R, Sloane BF, and Keppler D (2000) Inhibitors of papain-like cysteine peptidases, in *Handbook of Experimental Pharmacology* (von der Helm K, Korant BD, and Cheronis JC eds) Vol. 140, pp 301–328, Springer-Verlag, Berlin.

Stoka V, Turk B, Schendel SL, Kim T-H, Cirman T, Snipas SJ, Ellerby LM, Bredesen D, Freeze H, Abrahamson M, et al. (2001) Lysosomal protease pathways to apoptosis: cleavage of Bid, not pro-caspases, is the most likely route. *J Biol Chem* **276:**3149–3157.

Stypmann J, Gläser K, Roth W, Tobin DJ, Petermann I, Matthias R, Monnig G, Haverkamp W, Breithardt G, Schmahl W, et al. (2002) Dilated cardiomyopathy in mice deficient for the lysosomal cysteine peptidase cathepsin L. *Proc Natl Acad Sci USA* **99:**6234–6239.

Sulentic CEW, Holsapple MP, and Kaminski NE (2000) Putative link between transcriptional regulation of IgM expression by 2,3,7,8-tetrachlorodibenzo-*p*-dioxin and the aryl hydrocarbon receptor/dioxin-responsive enhancer signaling pathway. *J Pharmacol Exp Ther* **295:**705–716.

Terman A, Neuzil J, Kagedal K, Öllinger K, and Brunk UT (2002) Decreased apoptotic response of inclusion-cell disease fibroblasts: a consequence of lysosomal enzyme missorting? *Exp Cell Res* **274:**9–15.

Tobin DJ, Foitzik K, Reinheckel T, Mecklenburg L, Botchkarev VA, Peters C, and Paus R (2002) The lysosomal protease cathepsin L is an important regulator of keratinocyte and melanocyte differentiation during hair follicle morphogenesis and cycling. *Am J Pathol* **160:**1807–1821.

MOL PHARM
MOLECULAR PHARMACOLOGY
aspet
Downloaded from molpharm.aspetjournals.org by guest on December 1, 2012

Wang JL, Liu D, Zhang ZJ, Shan S, Han X, Srinivasula SM, Croce CM, Alnemri ES, and Huang Z (2000) Structure-based discovery of an organic compound that binds Bcl-2 protein and induces apoptosis of tumor cells. *Proc Natl Acad Sci USA* **97:**7124–7129.

Wei MC, Lindsten T, Nootha VK, Weiler S, Gross A, Ashiya M, Thompson CB, and Korsmeyer SJ (2000) tBid, a membrane-targeted death ligand oligomerizes BAK to release cytochrome c. *Genes Dev* **14:**2060–2071.

Werneburg NW, Guicciardi ME, Bronk SF, and Gores GJ (2002) Tumor necrosis factor-α-associated lysosomal permeabilization is cathepsin B dependent. *Am J Physiol Gastrointest Liver Physiol* **283:**G947–G956.

Whitlock JP Jr (1999) Induction of cytochrome P4501A1. *Annu Rev Pharmacol Toxicol* **39:**103–125.

Yuan X-M, Li W, Dalen H, Lotem J, Kama R, Sachs L, and Brunk UT (2002) Lysosomal destabilization in p53-induced apoptosis. *Proc Natl Acad Sci USA* **99:**6286–6291.

Address correspondence to: John J. Reiners, Jr., Institute of Environmental Health Sciences, Wayne State University, 2727 Second Ave., Room 4000, Detroit, MI 48201. E-mail: john.reiners.jr@wayne.edu

MOL PHARM

MOLECULAR PHARMACOLOGY

aspet

Downloaded from molpharm.aspetjournals.org by guest on December 1, 2012